Inorg. Chem. **2006**, *45*, 1192−1200

Toward Development of Water Soluble Dye Derivatized Nitrosyl Compounds for Photochemical Delivery of NO

Stephen R. Wecksler, Jordan Hutchinson,[1] and Peter C. Ford*

Department of Chemistry and Biochemistry, University of California, Santa Barbara, Santa Barbara, California 93106-9510

Received October 5, 2005

This report describes the synthesis, spectroscopy, and photochemistry of a new fluorescein-derivatized iron sulfur nitrosyl compound, the Roussin's red salt ester bis-((μ-S,μ-S′)-fluorescein-2-thioethyl-ester)-tetranitrosyldiiron (**Fluor-RSE**). Under continuous photolysis **Fluor-RSE** decomposes with moderate quantum yields (0.0036 ± 0.0005 at λ_{irr} = 436 nm) with the corresponding release of most of the NO carried by the $Fe_2S_2NO_4$ cluster. Large changes in the optical absorptivity occur upon photolysis of the **Fluor-RSE**, and these changes have been attributed to the different protic forms available to the fluorescein chromophore as it is separated from the cluster. Steady-state luminescence experiments have shown that the fluorescence of **Fluor-RSE** is about 85% quenched relative to the model compound ethyl fluorescein (**Fluor-Et**). Thus, it is clear that excitation of the fluorescein chromophore antennae is followed by energy transfer to the Fe/S/NO cluster at a rate at least comparable to fluorescence. However, the effect of the iron–sulfur core on the fluorescent lifetimes from fluorescein chromophore is much smaller. A single-exponential decay (τ = 3.3 ns) was seen for **Fluor-RSE** that is only modestly shorter than that for **Fluor-Et** (τ = 4.5 ns), and this is the effect of the smaller radiative rate constant (k_r) for the former. These systems further demonstrate that attachment of a pendant dye chromophore as an antenna significantly improves the effective rate for photochemical NO generation from the Roussin's red salt esters at longer excitation wavelengths.

Introduction

Nitrogen monoxide (generally called nitric oxide) has drawn considerable renewed interest since the discovery of its roles in mammalian biochemistry in the late 1980s. It is now well established that nitric oxide is the biological messenger responsible for vasodilatation, inhibits platelet aggregation, plays a role in immune response, and acts as a neurotransmitter.[2] NO has also been demonstrated to be a γ-radiation sensitizer and as such may prove useful in enhancing the effectiveness of radiation treatment for solid tumors.[3] In this regard, we have been concerned with the development of thermally stable, metal nitrosyl compounds that are capable of the photochemical generation of NO.[4] One type of system that has been explored for this purpose is based on the iron−sulfur−nitrosyl cluster compounds known as the Roussin's salts.[5] Photolysis of Roussin's black salt ($NH_4[Fe_4S_3(NO)_7]$, **RBS**) and Roussin's red salt ($Na_2[Fe_2(\mu\text{-}S)_2(NO)_4]$, **RRS**) in solution generates NO

* To whom correspondence should be addressed. E-mail: ford@chem.ucsb.edu.

(1) Visiting undergraduate researcher from the University of Sheffield, England.

(2) (a) Ignarro, L. J.; Buga, G. M.; Wood, K. S.; Byrns, R. E.; Chaudhuri, G. *Proc. Natl. Acad. Sci., U.S.A.* **1987**, *84*, 9265. (b) Palmer, R. M. J.; Ferrige, A. G.; Moncada, S. *Nature* **1987**, *327*, 524. (c) Palmer, R. M. J.; Ashton, D. S.; Moncada, S. *Nature (London)* **1988**, *333*, 664−666. (d) Azuma, H.; Ishikawa, M.; Sekizaki, S. *Br. J. Pharmacol*. **1986**, *88*, 411−415. (e) Radomski, M. W.; Palmer, R. M. J.; Moncada, S. *Br. J. Pharmacol* **1987**, *92*, 181−187. (f) Steuhr, D. J.; Marletta, M. A. *J. Immunol.* **1987**, *139*, 518−525. (g) Iyengar, R.; Stuehr, D. J.; Marletta, M. A. *Proc. Natl. Acad. Sci*. **1987**, *84*, 6369−6373.

(3) (a) Howard-Flanders, P. *Nature (London)* **1957**, *180*, 1191. (b) Thomlinson, R. H.; Gray, L. H. *Br. J. Cancer* **1995**, *9*, 539−549. (c) Powers, W. E.; Tolmach, L. J. *Nature (London)* **1963**, *197*, 710−711. (d) Mitchell, J. B.; Wink, D. A.; DeGraff, W.; Gamson, J.; Keefer, L. K.; Krishna, M. C. *Cancer Res*. **1993**, *53*, 5845−5848.

(4) (a) Hoshino, M.; Ozawa, K.; Seki, H.; Ford, P. C. *J. Am. Chem. Soc*. **1993**, *115*, 9568−9575. (b) Lorkovic, I. M.; Miranda, K. M.; Lee, B.; Bernhard, S.; Schoonover, J. R.; Ford, P. C. *J. Am. Chem. Soc.* **1998**, *120*, 11674−11683. (c) Hoshino, M.; Nagashima, Y.; Seki, H.; DeLeo, M.; Ford, P. C. *Inorg. Chem*. **1998**, *37*, 2464−2469. (d) De Leo, M.; Ford, P. C. *J. Am. Chem. Soc*. **1999**, *121*, 1980−1981. (e) Works, C. F.; Ford, P. C. *J. Am. Chem. Soc*. **2000**, *122*, 7592−7593. (f) Works, C. F.; Jocher, C. J.; Bart, G. D.; Bu, X.; Ford, P. C. *Inorg. Chem*. **2002**, *4*, 3728. (g) DeRosa, F.; Bu, X.; Ford, P. C. *Inorg. Chem*. **2003**, *42*, 4171−4178. (f) DeRosa, F.; Bu, X.; Ford, P. C. *Inorg. Chem*. **2005**, *44*, 4157−4165. (h) DeRosa, F.; Bu, X.; Pohaku, K.; Ford, P. C. *Inorg. Chem*. **2005**, *44*, 4166−4174.

(5) (a) Roussin, F. Z. *Ann. Chim. Phys*. **1858**, *52*, 285. (b) Butler, A. R.; Glidewell, C.; Li, M.-H. *Adv. Inorg. Chem*. **1988**, *32*, 335−393.

10.1021/ic051723s CCC: $33.50 © 2006 American Chemical Society
Published on Web 01/04/2006

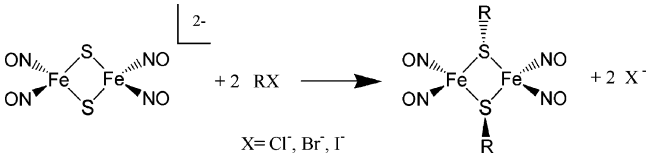

Figure 1. General synthetic scheme for the formation of the Roussin's red salt esters.

in moderate quantum yields upon UV−vis photolysis.[6] Follow-up studies on the latter demonstrated that **RRS** could act as the photochemical precursor of a radiation sensitizer, presumably NO.[7] In these experiments, hypoxic Chinese hamster V79 cell cultures were treated with the red salt then subjected to γ-radiation. In the absence of simultaneous photoexcitation by irradiation from the white light of a tungsten−halogen lamp, there was little difference in the survival rates of the red-salt-treated cells from the control (untreated) cells. However, when the cells treated with **RRS** were also subjected to white light photolysis, a marked decrease in cell survival was observed relative to the control. This markedly increased sensitivity to γ-radiation was attributed to the photochemical production of intracellular nitric oxide.

Although the Roussin's red and black salts proved to be effective photochemical NO generators, neither compound displays significant absorptivity at the longer visible-range wavelengths, and this property limits their in vivo applications. For this reason, we initiated the investigation of compounds known as the Roussin's red salt esters ($Fe_2(\mu\text{-}SR)_2(NO)_4$, RSE) as an alternative class of molecules for photochemical NO delivery drugs.[8−10] These compounds can be been prepared from the reaction of an alkyl halide with the red salt anion (Figure 1). In principle, it should be possible to utilize such an approach to design RSEs with the appropriate functionalities incorporated into the R− group to impart desirable optical and/or photochemical properties.

In this context, the "simple" RSEs (where R = CH_3, CH_2CH_2OH, $CH_2CH_2SO_3^-$) were prepared and their photochemical behaviors studied.[8] These display optical spectra similar to the parent **RRS** and have been shown to undergo photochemical decomposition with moderate quantum yields (at λ_{irr} = 366 nm, Φ = 0.02−0.23) in various solutions. It is significant that the esters release ∼4 mol of NO per mole of cluster upon UV−vis photolysis, in contrast to the behavior of aqueous solutions of **RRS**, which undergo photochemical conversion to the black salt with the net release of only one mole of NO for 2 mol of **RRS** undergoing this conversion.

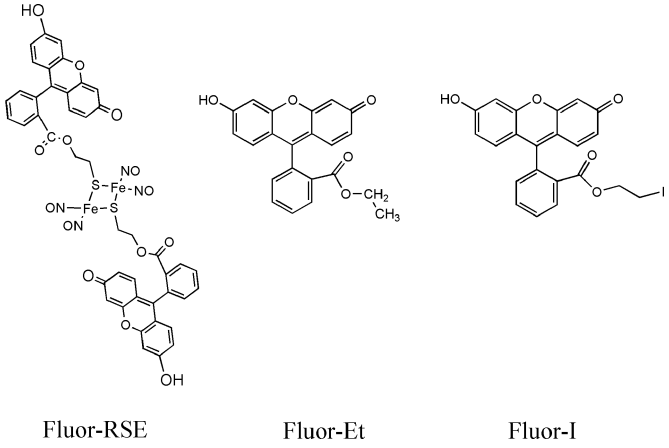

Fluor-RSE Fluor-Et Fluor-I

Figure 2. Formulas for **Fluor-RSE**, **Fluor-Et**, and **Fluor-I**.

The demonstration of NO release from the simple RSEs has implied that these compounds could serve as photodynamic therapy agents, but, like the red salt precursor, they have low absorptivities at longer excitation wavelengths where light penetration in tissue is maximized. To address this issue, an RSE was constructed in which the R groups are the dye protoporphyrin IX (PPIX).[9] The photochemistry and photophysics of the μ-S,μ-S′-protoporphyrin IX bis(2-thioethyl)diester]tetranitrosyldiiron complex (**PPIX-RSE**) were studied, and quantum yield measurements demonstrated that PPIX chromophore was capable of sensitizing NO release from the RSE at longer irradiation wavelengths (λ_{irr}). Further studies also demonstrated that **PPIX-RSE** could generate NO via two-photon excitation (TPE) at 800 nm.[10] One drawback of **PPIX-RSE** is that it shows little water solubility, and like the simpler RSEs, the quantum yield for NO release decreases with longer wavelengths. Therefore, alternative strategies have been pursued in order to develop water-soluble, dye-derivatized RSEs that can serve as photochemical NO generators via single and two photon excitation.

In the work described here, the red salt was derivatized with the well-known xanthene dye fluorescein to form the corresponding bis-[(μ-S,μ-S′)-difluorescein-thioethylester]-tetranitrosyl-diiron complex (**Fluor-RSE**) (Figure 2). Fluorescein and its derivatives have found broad application in biological imaging[11] with a focus recently on the development of fluorescein analogues derivatized with chelating functionalities for transition metal ion imaging.[12] Key characteristics of fluorescein, such as versatility in synthetic manipulation, strong extinction coefficients, high fluorescent quantum yields (Φ_f = 0.93), and water solubility make this an attractive compound for imaging applications.[13] These properties have also made fluorescein a candidate for two-photon excitation microscopy, and a large body of work has been undertaken to understand the photophysical properties

(6) (a) Bourassa, J.; Lee, B.; Bernard, S.; Schoonover, J.; Ford, P. C. *Inorg. Chem.* **1999**, *38*, 2947−2952. (b) Bourassa, J.; Ford, P. C. *Coord. Chem. Rev.* **2000**, *200*−*202*, 887−900. (c) Bourassa, J. L. Ph.D. Dissertation, U. C. Santa Barbara, 1998.
(7) Bourassa, J.; DeGraff, W.; Kudo, S.; Wink, D. A.; Mitchell, J. B.; Ford, P. C. *J. Am. Chem. Soc.* **1997**, *119*, 2853.
(8) (a) Conrado, C.; Bourassa, J.; Egler, C.; Wecksler, S.; Ford, P. C. *Inorg. Chem.* **2003**, *42*, 2288−2293. (b) Conrado, C. Ph.D. Dissertation, U. C. Santa Barbara, 2002.
(9) Conrado, C. L.; Wecksler, S.; Egler, C.; Magde, D.; Ford, P. C. *Inorg. Chem.* **2004**, *43*, 5543−5549.
(10) Wecksler, S.; Mikhailovsky, A.; Ford, P. C. *J. Am. Chem. Soc.* **2004**, *126*, 13566.
(11) (a) Smith, L. M.; Sanders, J. Z.; Kaiser, R. J.; Dodd, C.; Connell, C. R.; Heiner, C.; Kent, S. B. H.; Hood, L. E. *Nature* **1986**, *321*, 674. (b) Cheng, Y.; Dovichi, N. J. *Science* **1988**, *242*, 562. (c) Murchie, A. I. H.; Clegg, R. M.; von Kizing, E.; Duckett, D. R.; Diekmann, S.; Lilley, D. M. J. *Nature* **1989**, *341*, 763. (d) Chen, F. F. *Arch. Biochem. Biophys.* **1969**, *133*, 265−276. (e) Arbeloa, I. L. *J. Photochem.* **1980**, *14*, 97. (f) Guilford, J.; Xiaohua, Q. *J. Photochem. Photobiol., A: Chem.* **1998**, *113*, 125.

of this compound under single- and two-photon excitation.[14] The present report describes the synthesis and single-photon photochemistry of **Fluor-RSE**, along with comparative photophysical studies of other relevant fluorescein derivatives. In a subsequent manuscript, we will describe studies examining the properties of these molecules under two-photon excitation at near-infrared (NIR) wavelengths where light transmission through tissue is maximized.

Experimental Section

Materials. Fluorescein, 2-iodoethanol, dicyclohexylcarbodiimide, dimethylamino-pyridine, and 1-hydroxybenzotriazole were purchased from Aldrich and used without further purification. Sephadex LH-20 was purchased from Amersham Biosciences. Nanopure water was obtained for spectroscopic studies via a Millipore water purification system. Tetrahydrofuran (THF) was distilled under dinitrogen from sodium and benzophenone. Acetonitrile and methanol were distilled under dinitrogen from calcium hydride (CaH_2). Acetonitrile/phosphate buffer mixtures used for spectroscopic studies were prepared as follows. Phosphate buffers (1−10 mM) were prepared in Nanopure water, and their pH was adjusted to 7.4 using an Orion Research (model 701 A) digital ionalyzer. These solutions were then slowly diluted to a 50:50 mixture with distilled acetonitrile.

All gases were purchased from PRAXAIR, Inc. and used as received unless further specified. High-grade argon used for inert atmosphere preparation was passed through a Drierite/molecular sieve (4 Å) column to remove any remaining water. Deoxygenated solutions were prepared by sparging solutions with dinitrogen or argon for ∼1 min/mL. All inert atmosphere work was performed on a Schlenk line or in an inert (Ar) atmosphere glovebox (VAC atmospheric company, Nexus model). Deaerated solutions were prepared via three freeze−pump−thaw (f−p-t) cycles.

Instruments. UV−vis absorption spectra were measured using either a HP8572 diode array spectrophotometer or Shimadzu dual-beam UV-2401 PC spectrophotometer. All spectra were recorded in high-quality quartz UV−vis cells (NSG Precision Cells, Inc., Starna Cells) with 1 cm path lengths. Infrared spectra were obtained on a BioRad FTS 60 SPC 3200 FTIR spectrometer. Solution IR spectra were recorded in sealed cells (Reflex Analytical, Inc., International Crystal Labs) with a fixed path length of 0.05 or 0.02093 cm, CaF_2 windows, and a Teflon spacer and stoppers. Real-time detection of nitric oxide in solution was accomplished using an amiNO-700 electrode from Innovative Instruments, Inc. (Tampa, FL) capable of quantitatively detecting nanomolar concentrations of NO in aqueous solution. The electrode is calibrated from 50 to 400 nM in [NO] via injections of known quantities of nitrite standards into acidified solutions in the presence of a reducing agent.

Luminescence Measurements. Steady-state fluorescence spectra were recorded using a Spex Fluorolog 2 spectrofluorimeter with a 150 W xenon lamp excitation source. The resulting emission was collected at 90°. The excitation and emission beams were passed through SPEX 1681 Singlemate monochromators to isolate the appropriate wavelengths, and the emitted light was recorded with a Hamamatsu R928-A water-cooled PMT configured for single-photon counting and interfaced with a computer running Spex DM3000f software. The emission spectra were corrected for PMT response and deviations in lamp intensity by the ratio method using Rhodamine-6G as a standard. Samples were prepared in high-quality, four-sided quartz cuvettes (Starna cells) such that the absorbance at the excitation wavelength was less than 0.1. The photoluminescence quantum yield for **Fluor-Et** was determined by comparing the integrated fluorescent emission intensity referenced to fluorescein (in buffered solution at pH 11: $\epsilon = 7.69 \times 10^4\ M^{-1}\ cm^{-1}$ at $\lambda = 490$ nm, $\Phi = 0.93$).[13] The optical absorbance spectra (<0.1) were matched at the excitation wavelength ($\lambda_{ex} = 460$ nm), and the corresponding integrated fluorescence intensity was measured (from $\lambda_{mon} = 485-700$ nm) using a PTI fluorimeter.

Fluorescent lifetimes were measured using the time-correlated single-photon counting (TCSPC) technique at the UCSB Optical Characterization Facility. The samples were excited by near-UV ($\lambda_{ex} = 360-460$ nm) laser pulses with a duration of ∼120 fs, generated via second harmonic generation from the output of an ultrafast Ti:sapphire laser (Spectra Physics Tsunami). To avoid saturation of the chromophore, the repetition rate of the excitation pulses was reduced by a custom-built acousto-optical pulse picker. The luminescence was dispersed in a spectrometer and detected by a microchannel plate photomultiplier tube (MCP PMT; Hamamatsu R3809U-51). The triggering signal for the correlator board was generated by a fast photodiode illuminated via a beam splitter introduced into the excitation beam. MCP PMT output and triggering signal were connected to SPC-630 TCSPC board (Beker and Hickl) which performed the statistical analysis of the photon flux and restored the fluorescence transients. The instrument response function has fwhm ≈ 55 ps and is determined by the speed of MCP PMT response. Since the instrument response time is much shorter than the photoluminescence (PL) lifetime in the materials studied, deconvolution procedures to improve the temporal resolution of the system were not necessary.

Photochemical Experiments. The continuous photolysis experiments were performed using an optical train with an Oriel 200W Hg arc lamp in an Oriel model 66033 lamp housing as the excitation source, equipped with an Oriel model 68910 light intensity controller. The optical train also includes a water-filled cell for IR filtration, neutral density filters, and the appropriate interference filter (366 or 436 nm) to isolate the desired irradiation wavelength. The light intensity of the mercury arc lamp at $\lambda_{irr} = 366$ or 436 nm was determined by using the ferrioxalate actinometer.[15] Quantum yields (Φ) were calculated by monitoring changes in the optical absorption spectrum over a period of time. The sample solutions were placed in quartz cuvettes of 1.0 cm path length, stirred continuously, and kept from exposure to extraneous light. Known concentrations of samples were prepared in aerated solutions and irradiated for various periods of time.

(12) (a) Walkup, G. K.; Burdette, S. C.; Lippard, S. J.; Tsien, R. Y. *J. Am. Chem. Soc.* **2000**, *122*, 5644−5645. (b) Burdette, S. C.; Walkup, G. K.; Spingler, B.; Tsien, R. Y.; Lippard, S. J. *J. Am. Chem. Soc.* **2001**, *123*, 7831−7841. (c) Burdette, S. C.; Frederickson, C. J.; Bu, W.; Lippard, S. J. *J. Am. Chem. Soc.* **2003**, *125*, 1778−1787. (d) Nolan, E. M.; Burdette, S. C.; Harvey, J. H.; Hilderbrand, S. A.; Lippard, S. J. *Inorg. Chem.* **2004**, *43*, 2624−2635. (e) Chang, C. J.; Nolan, E. M.; Jaworski, J.; Okamoto, K.-I.; Hayashi, Y.; Sheng, M.; Lippard, S. J. *Inorg. Chem.* **2004**, *43*, 6774−6779. (f) Nolan, E. M.; Lippard, S. J. *Inorg. Chem.* **2004**, *43*, 8310−8317.

(13) (a) Weber, G.; Teale, F. W. J. *Trans. Faraday Soc.* **1957**, *53*, 646. (b) Hercules, D. M.; Frankel, H. *Science* **1960**, *131*, 1611. (c) Seybold, P. G.; Gouterman, M.; Callis, J. *Photochem. Photobiol.* **1969**, *9*, 229. (d) Sjöback, R.; Nygren, J.; Kubista, M. *Spectrochim. Acta Part A* **1995**, *51*, L7−L21.

(14) (a) Webb, W. W.; Xu, C. *J. Opt. Soc. Am. B* **1997**, *13*, 481−491. (b) Boguta, A.; Wróbel, D. *J. Fluoresc.* **2001**, *11*, 129−137. (c) Acemioğlu, B.; Arik, M.; Efeoğlu, H.; Onganer, Y. *J. Mol. Struct. (THEOCHEM)* **2001**, *548*, 165−171. (d) Alvarez-Pez, J. M.; Ballesteros, L.; Talavera, E.; Yguerabide, J. *J. Phys. Chem. A* **2001**, *105*, 6320−6332.

(15) (a) Calvert, J.; Pitts, J. In *Photochemistry*; J. Wiley and Sons: New York, 1967. (b) Hatchard, C.; Parker, C. *Proc. R. Soc. (London) A* **1956**, *235*, 518.

Syntheses. Fluorescein-2-iodoethyl Ester·Trifluoracetic Acid (Fluor-I·HTFA). A three-neck, round-bottom flask equipped with a stir bar and sealed with a septum was charged with a 0.664 g (0.002 mol) portion of spirit yellow fluorescein, and a 50 mL volume of dry distilled THF under inert atmosphere was added. After the dye was completely dissolved, 0.271 g of 1-hydoxybenztriazole (0.002 mol) and 0.025 g of 4-(dimethylamino)-pyridine ($\sim 10^{-5}$ mol) were added. The solution was cooled in an ice bath to 0 °C, and then 0.413 g of 1,3-dicyclocarbodiimide (DCC, 0.002 mol) was added slowly to the reaction flask. The reaction mixture was stirred in an ice bath for ~10 min before 0.18 mL of 2-iodoethanol (0.002 mol) was added dropwise via syringe. The reaction was stirred in an ice bath under argon for ~3 h at which point the solution was allowed to warm to room temperature and then was stirred overnight. The solution was filtered, and the residue was washed with THF in order to dissolve any remaining product. The solvent was then removed via rotary evaporation, and the remaining solid was extracted into ice-cold chloroform. The chloroform dissolves the **Fluor-I** product but not the dicyclohexylurea byproduct. This solution was then filtered via vacuum filtration, and the filter cake was washed with more cold chloroform. The solvent was removed via rotary evaporation.

The product was then further purified by column chromatography on silica gel using a $CHCl_3/CH_3OH$/trifluoroacetic acid (HTFA) mixture as the eluent. The third band to elute from the column is bright orange and was found to contain only the desired product. The solvent was removed via rotary evaporation, and the remaining compound was recovered as an oil. After this material was subjected to high vacuum, a bright orange-red crystalline solid was formed. The corresponding fluorescein-2-iodoethyl ester·trifluoroacetic acid adduct was isolated in a 26% yield (low yield due to the formation of the unreactive hydroxide-bound DCC-Fluor byproduct). The **Fluor-I**·HTFA product was identified by UV−vis, low- and high-resolution ESI MS, ^{1}H NMR, ^{19}F NMR, and ^{1}H/^{1}H COESY 2D NMR spectroscopy, and elemental analysis. UV−vis (CH_3OH) (λ_{max} in nm (ϵ in M^{-1} cm^{-1})): 380 (6.50×10^3), 432 (1.69×10^4), 466 (3.36×10^4), 502 (5.46×10^4). IR ($CHCl_3$) (ν_{CO} in cm^{-1}): 1725 (s). LRMS-ESI$^+$ (20% $CHCl_3$ in CH_3OH): *m/z* 487 ($[C_{22}H_{15}O_5I] + H^+)^+$, 509 ($[C_{22}H_{15}O_5I] + Na^+)^+$. LRMS-ESI$^-$ (20% $CHCl_3$ in CH_3OH): *m/z* 113 $(CF_3COO)^-$, 127 $(I)^-$, 485 $(C_{22}H_{14}O_5I)^-$. HRMS-ESI$^+$ (20% $CHCl_3$ in CH_3OH): Calcd 487.0037 ($[M] + H^+)^+$. Found 487.0053 ($[M] + H^+)^+$. ^{1}H NMR (in CD_3OD; δ, J = Hz): 2.94 (t, 5.6, 2H), 4.04 (t, 6, 2H), 6.94 (dd, 6, 2, 2H), 7.1 (s, 2H), 7.27 (dd, 9.2, 2, 2H), 7.29 (d, 7.2, 1H), 7.7 (m, 2H), 8.2 (d, 7.2, 1H). ^{19}F NMR (in CD_3OD; δ referenced to trifluorotoluene ($C_6H_5CF_3$): −10.1 (s). Anal. Calcd for $C_{22}H_{15}O_5I \cdot CF_3COOH$: C, 48.00%; H, 2.66%. Found (Marine Science Institute Analytical lab at UCSB): C, 47.72%; H, 2.72%.

Fluorescein-Ethyl Ester (Fluor-Et). The **Fluor-Et** compound was synthesized via a Fischer esterification reaction.[16] A 100 mL three-neck flask covered in aluminum foil, equipped with a stir bar and rubber septa, was charged with a solution of ~0.500 g of spirit yellow fluorescein (0.0015 mol) in 100 mL of gold seal 200 proof ethanol. To this solution, 5 mL of concentrated sulfuric acid (approximately 2 wt%) was added, and the solution was refluxed under air for 1 h. The solution was checked by ESI+MS and was still found to contain unreacted fluorescein. Therefore, the solution was refluxed for another hour at which time most of the reactant had been consumed. The solvent was removed via rotary evaporation, leaving a bright yellow solid. The compound was further purified on silica gel containing a $CHCl_3/CH_3OH$/triethylamine mixture. The first dark orange-yellow band to elute from the column was collected, and the solvent removed by rotary evaporation. The dried product was ~300 mg of purified material (percent yield = 55%). The compound was characterized by UV−vis, low- and high-resolution ESI$^+$ MS, ^{1}H NMR, and elemental analysis. UV−vis (in 50:50 CH_3CN/10 mM phosphate buffer in H_2O at pH 7.4) (λ_{max} in nm (ϵ in M^{-1} cm^{-1})): 240 (5.03×10^4), 258 (2.51×10^4), 322 (1.14×10^4), 472 (3.47×10^4), 504 (9.68×10^4). IR ($CHCl_3$) (ν_{CO} in cm^{-1}): 1717 (m). LRMS-ESI$^+$ (20% $CHCl_3$ in CH_3OH): *m/z* 361 ($[C_{22}H_{16}O_5] + H^+)^+$, 383 ($[C_{22}H_{16}O_5] + Na^+)^+$. HRMS-ESI$^+$ (20% $CHCl_3$ in CH_3OH): Calcd 361.10705 ($[M] + H^+)^+$. Found 361.1078 ($[M] + H^+)^+$. ^{1}H NMR (in $CDCl_3$, δ, J in Hz): 1.05 (t, 6.8, 3H), 4.03 (q, 6.8, 2H), 7.21 (d, 2, 1H), 7.23 (d, 2, 1H), 7.33 (s, 1H), 7.36 (s, 1H), 7.37 (d, 1.6, 1H), 7.52 (s, 1H), 7.83 (m, 2H), 8.36 (d, 1.2, 1H), 8.38 (d, 1.2, 2H). Anal. Calcd for $C_{22}H_{16}O_5$: C, 73.3%; H, 4.44%. Found: C, 71.98%; H, 4.41%.

Bis(μ-S-fluorescein-2-thioethyl-ester)tetranitrosyldiiron·Trifluoroacetic Acid (Fluor-RSE·HTFA). A 100 mL three-neck flask covered in aluminum foil, equipped with a stir bar and rubber septa, was charged with a solution of 0.682 g of **Fluor-I** (0.0014 mol) in 50 mL of dry, distilled THF. This solution was blanketed with argon and stirred until the compound was fully dissolved. To this solution 0.340 g of $Na_2[Fe_2S_2(NO)_4]\cdot 8H_2O$ (**RRS**) (0.0007 mol) was added to the mixture under inert gas. After the round-bottom flask was purged with argon, the mixture was allowed to stir in the dark overnight. After 24 h, the reaction mixture was checked for completion by recording the ESI+ MS. If the solution still contained unreacted **Fluor-I** at this point, approximately 100 mg of **RRS** was added to the reaction mixture in order to force the reaction to completion. The solution was left to stir under argon for another 24 h and then checked again by ESI+ MS. When all the **Fluor-I** was determined to be consumed, the reaction was stopped, and the solvent was removed via rotary evaporation.

The compound was then extracted several times with 100 mL of a $CHCl_3/CH_3OH$ mixture. The dark red-orange solutions were combined and then reduced to a minimum volume on the rotary evaporator. The solid was then resuspended in the $CHCl_3/CH_3OH$ mixture and further purified by column chromatography (silica gel $CHCl_3/CH_3OH$/HTFA). The first dark orange band to elute from the column was collected, and the solvent was removed via rotary evaporation. This material was observed to contain minor impurities, so the mixture was further purified by size exclusion chromatography on Sephadex LH-20 (Amersham Biosciences) in a $CHCl_3/CH_3OH$/HTFA mixture. The first dark orange band to elute from the column was collected, and the solvent removed by rotary evaporation. The compound can be recrystallized by ether diffusion into a deoxygenated methanol solution. The final product was isolated in ~15% yield. The light orange solid was then characterized via UV−vis, IR, low- and high-resolution ESI MS, ^{1}H NMR and ^{19}F NMR spectroscopy, and elemental analysis. UV−vis (in 50:50 CH_3CN/phosphate buffer (10 mM) H_2O pH 7.4) (λ_{max} in nm (ϵ in $M^{-1}cm^{-1}$)): 240 (5.30×10^4), 320 (1.15×10^4), 506 (7.22×10^4). IR (CH_3OH) (ν_{NO} in cm^{-1}): 1754 (s), 1781 (s), and 1810 (w). LRMS-ESI$^+$ (20% $CHCl_3$ in CH_3OH): *m/z* 508 ($[(C_{22}H_{15}O_5)_2 Fe_2S_2(NO)_4] + 2H^+)^{2+}$, 1015 ($[(C_{22}H_{15}O_5)_2 Fe_2S_2(NO)_4] + H^+)^+$, 1037 ($[(C_{22}H_{15}O_5)_2 Fe_2S_2(NO)_4] + Na^+)^+$. LRMS-ESI$^-$ (20% $CHCl_3$ in CH_3OH): *m/z* 1013 ($[(C_{22}H_{15}O_5)_2 Fe_2S_2(NO)_4] - H^+)^-$, 113 (trifluoroacetate, $(CF_3COO)^-$. HRMS-ESI$^+$ (20% $CHCl_3$ in CH_3OH): Calcd. 1014.9977 ($[M] + H^+)^+$. Found 1014.9992 ($[M] + H^+)^+$. ^{1}H NMR (in *d*-DMSO; δ, J in Hz): 2.94 (d, 5.6, 4H), 4.22 (t, 6.4, 2H), 4.27 (t, 5.2, 2H), 6.48 (s, 4H), 6.52 (d, 8.8, 4H), 6.82 (d, 9.2, 4H), 7.51 (d, 7.6, 2H), 7.85 (m, 4H), 8.29 (d, 6.4, 2H), 8.32 (s, 2H). ^{19}F NMR (in $CDCl_3$; δ referenced to trifluoro-

(16) March, J. *Advanced Organic Chemistry*, 4th ed.; John Wiley and Sons: New York, 1992.

Scheme 1. Synthetic Scheme for the Formation of **Fluor-RSE**

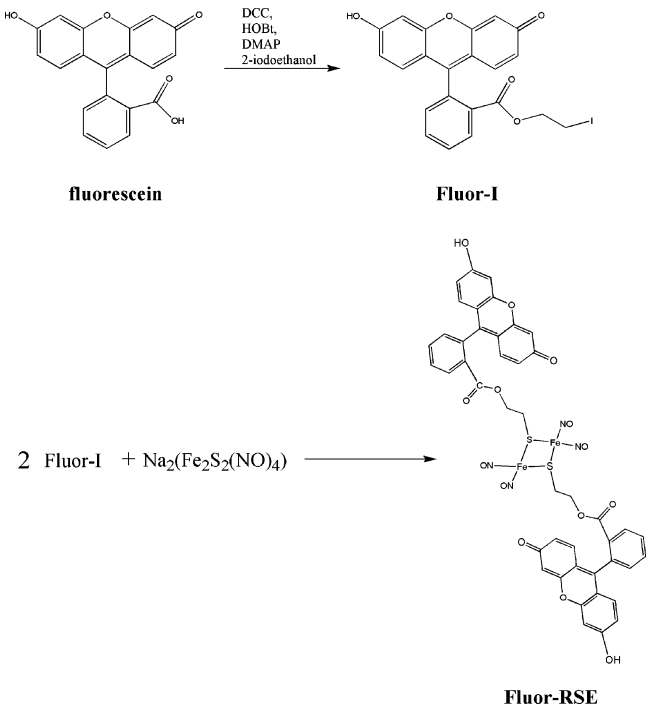

toluene ($C_6H_5CF_3$)): −10.0 (s). Anal. Calcd for $(C_{22}H_{15}O_5)_2Fe_2S_2(NO)_4 \cdot 2CF_3COOH$: C, 46.38%; H, 2.50%; N, 4.51%. Found: C, 46.12%; H, 2.55%; N, 4.38%.

The iron content in the same sample was determined using a Shimadzu AA 6200 atomic absorption flame emission spectrophotometer with iron calibration curves generated with dried 99.9% Fe_2O_3 (Aldrich) digested in hot nitric acid and diluted in Nanopure water to appropriate concentrations (5−75 ppm). The Fe content was found to be 9.4 (±0.7)%, in agreement with the theoretical value (9.02%).

Results and Discussion

Synthesis and Characterization of the Fluor-RSE. The synthetic scheme shown in Figure 1 describes the general procedure used for the formation of the Roussin's RSEs. Fluorescein dye contains a carboxylic acid functionality that can be readily substituted to form an ester with a pendant alkyl halide arm. The key step in the formation of the iodo-derivatized fluorescein precursor **Fluor-I** is the reaction of fluorescein with DCC in the presence of a base. This well-known procedure in peptide synthesis yields an activated O-acyl urea intermediate, which reacted with 2-iodoethanol to form **Fluor-I**. Reaction of this bright orange complex in a 2:1 ratio with the red salt gave the corresponding **Fluor-RSE** complex over a period of several days. The purification conditions utilized for **Fluor-RSE** (and the **Fluor-I** precursor) resulted in the isolation of the compounds as an HTFA adduct, which is further supported via analytical characterization using ^{19}F NMR, ESI-MS, and elemental analysis data. Of note is that all photochemical and photophysical measurements of **Fluor-RSE** were run in buffered media, ensuring that the pH of the solution was not affected by the HTFA adduct. X-ray-quality crystals of **Fluor-RSE** have not been obtained, but the IR, NMR, high-resolution MS spectra and elemental analysis are all consistent with the formulations of **Fluor-RSE** depicted in Scheme 1.

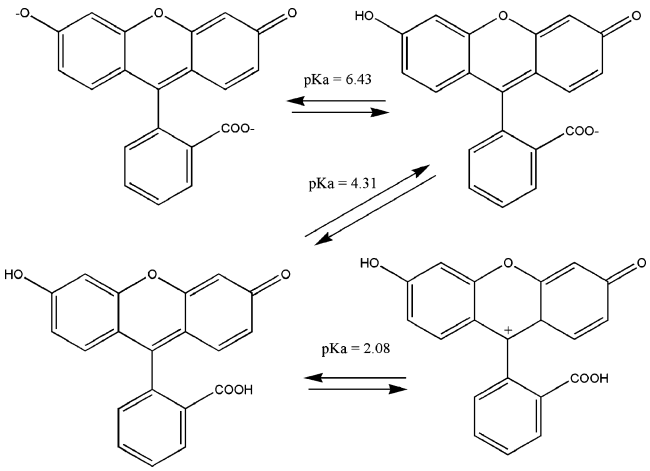

Figure 3. Protic equilibrium forms of fluorescein.

The IR spectrum of **Fluor-RSE** in methanol shows three distinct bands in the nitrosyl stretching region (ν_{NO}) at 1754 (s), 1781 (s), and 1810 cm^{-1} (w), consistent with that found for other RSEs.[9] The UV−vis spectrum of this compound in methanol is similar to that of the fluorescein precursor, but the main absorption band (at 506 nm) is red-shifted by 10 nm. Earlier studies of the photophysical properties of fluorescein have demonstrated that the optical spectrum is altered by the solvent conditions, buffer strength, and pH.[12−14] Fluorescein can exist in several protic forms dependent on pH and solvent conditions, with each conjugate having a different absorption spectrum, extinction coefficients, and photoluminescence quantum yields. For instance, at neutral pH (in 50:50 CH_3CN/phosphate buffer (10 mM) and pH 7.4), fluorescein is present in two forms, a monoanion and a dianion, and has an absorption maximum of 496 nm ($\epsilon = 6.95 \times 10^4$ M^{-1} cm^{-1}). For comparison, under identical conditions, **Fluor-RSE** has a λ_{max} at 506 nm with $\epsilon = 7.22 \times 10^4$ M^{-1} cm^{-1}; however, since **Fluor-RSE** has two fluorescein moieties, the ϵ per chromophore is half that value.

Since fluorescein spectral properties are not only affected by solvent conditions and pH but (as shown above) also by synthetic modification of the chromophore, it was desirable to have a model compound (**Fluor-Et**) for comparison to the polychromophoric complex **Fluor-RSE**. Although the synthesis of **Fluor-Et** has been reported,[17] the synthetic and purification procedures and characterization used here are described in detail, owing to the importance of this compound's purity for comparing the photophysical properties. The UV−vis absorbance spectra of fluorescein, **Fluor-RSE**, and **Fluor-Et** are compared in Figure 4. From these spectra (Table 1), it is apparent that the spectral properties of **Fluor-Et** resemble those of the **Fluor-RSE** with the exception of the shorter UV−vis wavelengths affected by transitions of the **RSE** chromophore.

Photochemical Studies. Fluor-RSE is quite stable under deoxygenated conditions and in the dark but undergoes photochemistry when irradiated in the presence of oxygen. This compound is but modestly soluble in aqueous buffer

(17) (a) Quick, J.; Otersor, R. *Tett. Lett.* **1977**, 599. (b) He, J.; Chen, F.; Zhao, J.; Hidaka, H. *Colloids Surf., A* **1998**, *142*, 49−57.

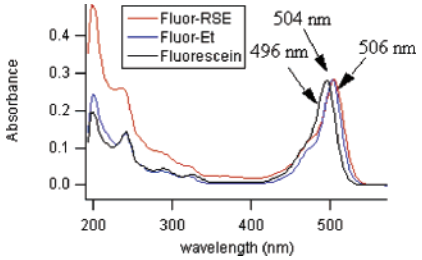

Figure 4. Electronic absorbance spectra of fluorescein (4.03 μM), **Fluor-RSE** (3.92 μM), and **Fluor-Et** (2.89 μM) in aerated solutions of 50:50 CH_3CN/phosphate buffer (10 mM) at pH 7.4.

Table 1. Spectroscopic Properties of Fluorescein, **Fluor-Et**, and **Fluor-RSE** in a 50:50 Mixture of CH_3CN/Phosphate Buffer (10 mM) at pH 7.4

compound	absorbance λ_{max}	ϵ (M^{-1} cm^{-1})	emission λ_{max}	PL quantum yield (Φ_{PL})
Fluor-RSE	506 nm	7.2×10^4	528 nm	0.11 ± 0.03[a] (0.15 ± 0.02)[18]
Fluor-Et	504 nm	9.7×10^4	526 nm	0.77 ± 0.02
Fluorescein	496 nm	6.9×10^4	518 nm	0.93[b]

[a] PL quantum yield determined from steady-state luminescence measurements using the relative integrated fluorescence intensities of **Fluor-RSE** compared to **Fluor-Et**. Samples were prepared with matched absorbance (<0.1) at the excitation wavelength (λ_{exc} = 480 nm), with the integrated emission intensities determined from λ_{mon} 485−700 nm. [b] PL quantum yield determined for the fluorescein dianion in aqueous solution at pH 11.[13]

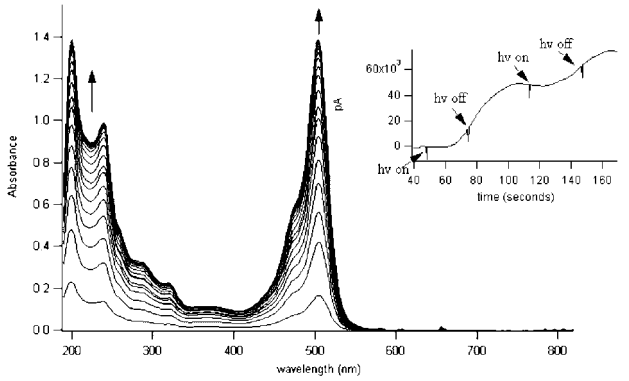

Figure 5. Optical spectra changes observed upon continuous wave photolysis (λ_{irr} = 436 nm) of **Fluor-RSE** (2.3 μM) in 50:50 CH_3CN/phosphate aerated buffer (10 mM) at pH 7.4. Inset depicts corresponding NO detection with an NO specific electrode.

solution at pH 7.4 but is quite soluble in a 50:50 mixture of acetonitrile and aqueous buffer solution at physiological pH. The quantum yields for the photodecomposition of **Fluor-RSE** were therefore measured in aerated solutions of 50:50 CH_3CN/phosphate buffer (10 mM) at pH 7.4. Quantum yields for photodecomposition were measured by monitoring the changes that occurred in the UV−vis spectrum upon photolysis. Immediately upon irradiation with 366 or 436 nm light, a large growth in optical absorptivity occurs across the UV−vis spectrum. The main peak at 506 nm grows and shifts to 504 nm within the first few minutes of irradiation. The photolysis-induced changes in the optical absorbance spectrum of the **Fluor-RSE** solutions upon UV−vis irradiation are shown in Figure 5.

The large changes observed in the absorbance spectrum upon photolysis of the **Fluor-RSE** were unexpected since continuous photolysis studies of the **PPIX-RSE** complex resulted in minimal changes in the optical absorption spectrum.[9] The pendant dye dominates the absorption spectrum of the **PPIX-RSE**, and the photoproduct absorption spectrum and extinction coefficients are nearly identical to the starting complex. For **Fluor-RSE**, however, the photoproducts exhibit significantly higher optical absorptivities than does the intact polychromophoric system, owing to the rather low extinction coefficients per dye unit for the latter. We have no ready explanation for this phenomenon other than to note that the absorptivity of fluorescein itself is markedly sensitive to the solution pH, owing to the differences between the monoanionic and dianionic forms; thus, the spectra differences may be due to shifts in the pK_a of chromophore between **Fluor-RSE** and the fluorescein−ethyl thiolate photoproduct.

The quantum yields for photodecomposition of **Fluor-RSE** (Φ_d) were measured from the optical spectrum changes. For λ_{irr} 366 and 436 nm, the Φ_d were found to be 0.022 ± 0.003 ($I_a = 1.1 \times 10^{-6}$ einstein/L·s) and 0.0036 ± 0.0005 (1.4×10^{-6} einstein/L·s), respectively, where I_a is absorbed light intensity. These can be compared to Φ_d values measured previously[8,9] for the photodecomposition of other RSEs and of **PPIX-RSE**; for example, $\Phi_d = 3.2 \times 10^{-4}$ (3.0×10^{-6} einstein/L·s) for $Fe_2(\mu\text{-}SCH_2C_6H_5)_2(NO)_4$ (**benzyl-RSE**) and $\Phi_d = 5.2 \times 10^{-4}$ (3.0×10^{-6} einstein/L·s) for **PPIX-RSE** in aerated, ambient temperature $CHCl_3$ at λ_{irr} = 436 nm. The quantum yield for photodecomposition at λ_{irr} = 436 nm is approximately an order of magnitude greater for **Fluor-RSE** than for **PPIX-RSE**, although it should be noted that the solvent systems are different.

The inset of Figure 5 shows the change in response of an NO-specific electrode upon UV−vis photolysis of **Fluor-RSE** in the mixed solvent. Immediately upon photolysis of the solution, a substantial increase in current is detected by the electrode, consistent with the photochemical production of NO from the dye-derivatized RSE. Quantitative electrochemical NO detection demonstrates that, like the simple RSE complexes, these complexes release most (3.2 ± 0.4) of their NO equivalents upon photodecomposition.

Further characterization of the photoproducts was also obtained by mass spectrometry of photolyzed **Fluor-RSE** solutions. In these experiments, aerated solutions of **Fluor-RSE** (6.6 μM) were dissolved in a 50:50 CH_3CN/Nanopure H_2O mixture, and irradiated at 436 nm for 1 min intervals. Then, 250 μL aliquots were withdrawn from the photolyzed solutions, kept from exposure to extraneous light, and injected in the ESI mass spectrometer operating in positive-ion mode. Before photolysis, only two peaks were observed in the spectrum at *m*/*z* 1015 and 508, corresponding to the singly $([M] + H^+)^+$ and doubly charged $([M] + 2H^+)^{2+}$ protonated parent ions, respectively. After 1 min of photolysis, several new peaks appeared in the spectrum and the relative intensity of the peaks at *m*/*z* 1015 and 508 diminished. After 2 min of photolysis, the peaks associated with the intact cluster nearly completely disappeared and a peak at *m*/*z* 393 began to dominate the spectrum. The peak at *m*/*z* 393 showed no iron isotope pattern but fit nicely with that of the protonated fluorescein-ethyl thiolate species (Fluor−

$CH_2-CH_2-SH + H^+)^+$. Within 5 min of irradiation, the peaks assigned to the parent ions were completely gone, and the spectrum only contained the species at *m*/*z* 393. This observation is consistent with analysis of the photochemical products of the simple RSE complexes, which demonstrated the formation of free thiols from photolysis of these clusters.[8]

Attempts at quantifying the iron photochemical products yielded inconclusive results, as the spectrophotometric assays used for this analysis met significant interference due to the strongly absorbing fluorescein chromophore. Nonetheless, the NO electrode and mass spectrometry experiments demonstrate that the dye-derivatized RSE complexes undergo photochemical reactions quantitatively and qualitatively similar to the simple RSE analogues where the absorbing chromophore is the Fe/S/NO cluster itself. Quantitatively, NO production from **Fluor-RSE** displays a larger Φ_d than the simpler RSE compounds, so it is clear that the fluorescein chromophore is serving as an antenna to capture the excitation energy and sensitize the photoreactivity of the cluster.

Emission Studies. Although the quantum yield for **Flour-RSE** ($\lambda_{irr} = 436$ nm) is larger than that measured for other RSE clusters, the relatively low quantum yield for photodecomposition raises questions regarding the efficiency of energy transfer occurring from the fluorescein to the iron sulfur nitrosyl core. This was evaluated by examining the steady-state luminescence quantum yields and the fluorescence lifetimes. In the quantum yield experiments, solutions of **Fluor-RSE** (1.88 μM) and **Fluor-Et** (1.80 μM) were prepared under deoxygenated conditions in 50:50 CH_3CN/phosphate buffer (10 mM) at pH 7.4 such that the absorbances ($\sim$0.1) at the excitation wavelength were matched. The samples were illuminated at $\lambda_{ex} = 480$ nm, while the emission was monitored over the λ_{mon} range 485−700 nm. Both samples displayed fluorescence in this range, but the integrated emission intensities of the two compounds indicated that the **Fluor-RSE** emission intensity was only 15% that of **Fluor-Et**. The significant quenching of **Fluor-RSE** relative to **Fluor-Et** demonstrates that the intramolecular energy transfer from the fluorescein chromophore to the RSE chromophore effectively competes with the radiative deactivation of the fluorescein excited state.

It is possible that the residual fluorescence is not an inherent property of **Fluor-RSE** but instead is due to a brightly emissive impurity left in the sample in significant concentrations by the synthetic procedure or formed by sample decomposition. The first possibility is challenged by the spectroscopic and physical evidence supporting the purity of the compound. Furthermore, several independent syntheses, recrystallizations, and solution preparations all gave materials with the same emission intensity relative to the **Fluor-Et** solutions. Thermal decomposition during sample preparation is more plausible since such decomposition of the **Fluor-RSE** compound does result in transformations to species with stronger fluorescence. However, careful sample preparation, handling, and fluorescence measurements under deoxygenated conditions resulted in little to no change in the emission spectrum even over extended time periods.

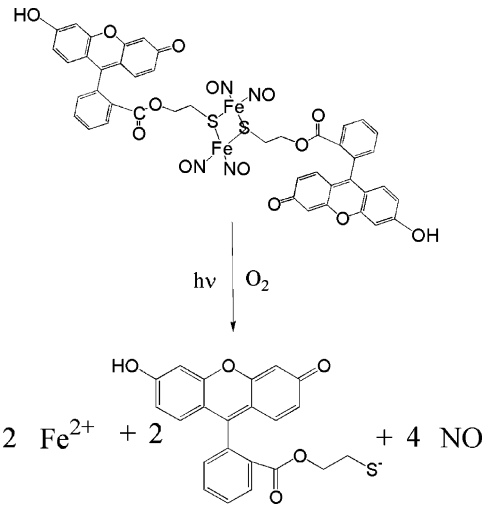

Figure 6. Scheme for the photochemical decomposition of the **Fluor-RSE**.

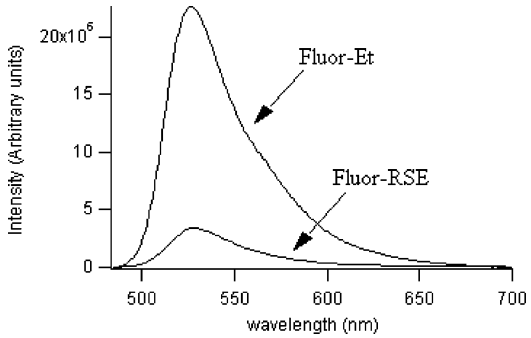

Figure 7. Fluorescence spectrum of **Fluor-Et** (1.80 μM) and **Fluor-RSE** (1.88 μM) in deoxygenated solutions of 50:50 CH_3CN/phosphate buffer (10 mM) at pH 7.4 under argon. Samples were prepared such that the absorbance at the excitation wavelength ($\lambda_{exc} = 480$ nm) were equal ($\sim$0.1).

Thus, we conclude that the residual emission is indeed an inherent photophysical property of **Fluor-RSE** and that pathways introduced by the RSE cluster that lead to deactivation of the fluorescent excited state are about six times as fast as the radiative rate constant, k_r, of that compound.

To evaluate these rate constants quantitatively, fluorescent lifetimes of the relevant species were measured using the single-photon counting technique described in the Experimental Section. In these experiments, solutions of **Fluor-RSE** and **Fluor-Et** were prepared under argon in 50:50 CH_3CN/phosphate buffer (1 mM) at pH 7.4 such that their absorbance at the excitation wavelength were less than 0.1. The solutions were excited at $\lambda_{exc} = 460$ nm, and the fluorescence traces were monitored at 532 nm. High-quality exponential decays were observed for each case. In this manner, the fluorescent lifetime for the **Fluor-Et** ester under deoxygenated conditions was found to be $\tau = 4.40 \pm 0.15$ ns, in good agreement with the published value ($\tau = 4.76$ ns in ethanol).[17] Under the same conditions, the measured lifetime for **Fluor-RSE** was $\tau = 3.29 \pm 0.25$ ns. The decay trace for **Fluor-RSE** is shown Figure 8.

It is obvious from comparing the lifetime data for **Fluor-RSE** and **Fluor-Et** that τ is significantly less affected by appending the fluorescein dye to the metal cluster than is the emission intensity. If the changes were due solely to

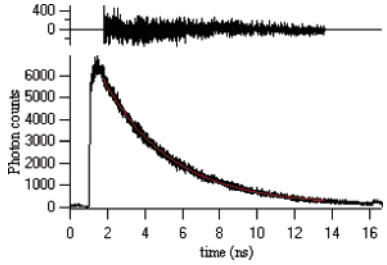

Figure 8. Fluorescence decay trace of **Fluor-RSE** (3.92 μM) in 50:50 CH_3CN/phosphate buffer (1 mM) at pH 7.4 under Ar. Trace is fit to a single exponential (shown in red) with residual scatter to the fit shown above.

quenching by energy transfer to the iron sulfur core, then the ratio of the fluorescent lifetimes should be equal to that of the ratio of the steady-state emission intensities, that is, $I_f/I'f' \cong \tau_f/\tau'f'$. However, this is clearly not the case, since the ratio of the fluorescent lifetimes measured for the **Fluor-RSE** and **Fluor-Et** is ~0.75, significantly larger than the ratio of intensities determined in the steady-state luminescence experiments (~0.15). The difference can be attributed to changes in the other rate constants, specifically the radiative rate constant from the fluorescein chromophore (k_r). The fluorescence quantum yield can be described by eq 1,

$$\Phi_f = k_r\tau_f \qquad (1)$$

and from the respective Φ_f (Table 1) and τ_f (above) values the radiative rate constants can be calculated from the relationship $k_r = \Phi_f\tau_f^{-1}$. These are k_r(Fluor-Et) = 1.75×10^8 s^{-1} and k_r(Fluor-RSE) = 3.3×10^7 s^{-1}. Thus, k_r is also strongly perturbed by formation of the trichromophoric complex and is about 4-fold smaller for **Fluor-RSE** than for **Fluor-Et**.

The different values for k_r must reflect a large difference in the transition dipole moment changes for the fluorescence processes of the two species. This is completely consistent with the differences in oscillator strengths for the visible-range absorption bands of these compounds. The respective bands for fluorescein and **Fluor-Et** are both significantly more intense than that for **Fluor-RSE** (Table 1). (If the spectrum of **Fluor-RSE** is due to the summed absorbances of two fluorescein chromophores, then $\epsilon = 3.6 \times 10^4$ M^{-1} cm^{-1} for each at the 506 nm λ_{max}, while that for **Fluor-Et** under these conditions is much larger at 9.7×10^4 $M^{-1}cm^{-1}$ at its 504 nm λ_{max}). The extinction coefficients reflect the oscillator strengths for analogous transitions, which in turn define the magnitudes of the radiative rate constants k_r.[19]

(18) The fluorescence quantum yield for **Fluor-RSE** was also determined independently, on a separate instrument (PTI fluorimeter) by Dr. Alexander Mikhailovsky of the Optical Characterization Facility at UCSB. In these measurements, the PL quantum yield was determined by comparing the relative integrated intensity of **Fluor-RSE** compared to that of fluorescein (in buffered solution at pH 11, $\epsilon = 7.69 \times 10^4$ M^{-1} cm^{-1} at $\lambda = 490$ nm, $\Phi = 0.93$).[13] The optical absorbance spectra (<0.1) were matched at the excitation wavelength (λ_{exc} = 460 nm), and the corresponding integrated fluorescence intensity was measured from λ_{mon} = 485−700 nm. For self-consistency, the quantum yield values used for the rate constant calculations were those determined from the relative measurement referenced to **Fluor-Et**, but it should be noted that difference in the quantum yields is close to the experimental uncertainty in the measurements. Using the higher value of Φ_f would give a calculated k_r(Fluor-RSE) of (4.5 ±1) × 10^7 s^{-1}.

Thus, if the fluorophores of the former are acting independently, the radiative rate constants from the individual fluorescein moieties of **Fluor-RSE** are much smaller than the k_r from **Fluor-Et**, and this was indeed experimentally shown. For this reason, it is not surprising that the ratio of the fluorescence lifetimes for these two compounds is much larger than the ratio of the steady-state emission intensities.

On the basis of the k_r value and Φ_r determined above for **Fluor-RSE** and **Fluor-Et**, one can use eqs 2 and 3 to estimate a $k_{q'}$

$$\tau_f\,(\text{Fluor-Et}) = (k_r(\text{Fluor-Et}) + k_{nr} + k_{isc})^{-1} \qquad (2)$$

$$\tau_f(\text{Fluor-RSE}) = (k_r(\text{Fluor-RSE}) + k_{nr'} + k_{isc'} + k_{q'})^{-1} \qquad (3)$$

value of 2.23×10^8 s^{-1} where k_{nr} and k_{isc} are the respective rate constants for nonradiative decay to the ground state and for intersystem crossing to the triplet excited state and $k_{q'}$ is the rate constant for intramolecular energy transfer from the fluorescent excited state of the pendant chromophores to the $Fe_2S_2(NO)_4$ cluster. Such an estimate requires the assumption that the nonradiative deactivation and intersystem crossing rate constants are the same for the two systems, an assumption that seems risky given the marked perturbation of the radiative rate constants. On the other hand, given that the Φ_d and Φ_{NO} values measured for **Fluor-RSE** are at least comparable to the values measured under similar conditions for the simple RSE clusters,[9] it seems unlikely that these other pathways are playing a major role in the deactivation of the appended fluorescein chromophore.

The steady-state luminescence experiments have demonstrated that efficient energy transfer occurs to the iron/sulfur/nitrosyl core upon the absorption of a photon by the fluorescein chromophores, and the Φ_d and Φ_{NO} values measured for **Fluor-RSE** demonstrate that the photochemical efficiency of NO production is not diminished by the attachment of the chromophore to the cluster. The fluorescein antenna is a much stronger chromophore than the simple RSE at visible-range wavelengths, and thus, **Fluor-RSE** more efficiently absorbs light at longer wavelengths, resulting in enhanced net photochemistry. The greater photochemical efficiency for **Fluor-RSE** can be illustrated by the following example. A sample of **Fluor-RSE** with an absorbance of 1.0 at λ_{max} = 504 nm gives a concentration of 1.39×10^{-5} M (in a 1-cm path length cell) and would have absorbance of 0.13 at the excitation wavelength used in the photochemical measurements (436 nm). A solution of $Fe_2(\mu\text{-}SCH_2CH_2OH)_2(NO)_4$ (bis(2-hydroxyethyl)-RSE) at the same concentration, would have absorbances of 0.05 at 436 nm and 0.009 at 504 nm.[8] The rate of NO production can be defined in terms of the intensity of the absorbed light (I_a, where $I_a = I_o(1 - 10^{-abs})$, according to the equation

$$\frac{d[NO]}{dt} = \Phi_{NO}I_a.$$

(19) Turro, N. J. *Modern Molecular Photochemistry*, University Sci. Books: Sausalito, CA, 1991.

Thus, at a fixed incident light intensity (I_o) and at similar concentrations, the rate of NO production for **Fluor-RSE** would be about 2.5 times greater than the simple RSE at 436 nm, and ~100 times greater at 504 nm.

Summary

The synthesis, spectroscopy, and photochemistry of a water-soluble fluorescein-derivatized RSE are described. This new polychromophoric compound acts as an effective photochemical NO generator with a moderate yield for photodecomposition ($\Phi_d = 0.0036$ for 436 nm irradiation ($I_a = 1.4 \times 10^{-6}$ einstein/L·s)). Quantitative NO electrode measurements have indicated that the compounds release ~3.2 mol of NO per cluster upon irradiation with UV−vis light, resembling parallel photochemistry of the simple RSE analogues. The large changes in optical absorptivity upon photolysis of **Fluor-RSE** indicates that the photophysics of this compound are significantly perturbed by attachment of the iron sulfur nitrosyl core, and this has been attributed to the different protic forms available to the fluorescein chromophore. Steady-state luminescence experiments have shown that the fluorescein chromophores on **Fluor-RSE** act as antennae for light harvesting, with the **Fluor-RSE** emission quenched by 85% comparatively to **Fluor-Et**. Temporal fluorescence decay measurements of **Fluor-RSE** display a single lifetime of 3.3 ns, slightly shorter than that (4.5 ns) of **Fluor-Et**. Differences in the ratios of the steady-state luminescence intensities and lifetimes for **Fluor-RSE** and **Fluor-Et** are attributed to differences in the effective radiative rate constants of the two compounds.

The present system again demonstrates that chromophore-linked Roussin's RSEs can be utilized for the photogeneration of NO and that the visible range absorbing pendant dye increases the effective rate of NO production. The **Fluor-RSE** system, which is considerably more aqueous compatible than previously described RSEs[9,10] draws closer to the possible therapeutic applications of such compounds.

Acknowledgment. These studies were supported by the National Science Foundation (CHE-0352650). We also thank Dr. Alexander Mikhailovsky of the UCSB Optical Characterization Facility for help in performing the fluorescence lifetime measurements and PL quantum yields.

IC051723S